



TREE-RING RECONSTRUCTION OF JUNE-JULY MEAN TEMPERATURES IN THE NORTHERN DAXING’AN MOUNTAINS, CHINA

YANGAO JIANG^{1,3}, YU WANG^{1,6}, JUNHUI ZHANG³, SHIJIE HAN^{2,3}, CASSIUS E.O. COOMBS⁴,
MARICELY ESCOBEDO⁴, JUNWEI WANG¹, XIAOGUANG WANG⁵, LIN HAO^{1,6}, GUODE LI¹,
YIJIANG TONG⁷, YUE GU³, SHENGZHONG DONG¹, HAISHENG HE¹ and JINGYU YANG¹

¹Experimental Teaching Center, Shenyang Normal University, Shenyang 110034, China

²School of Life Sciences, Henan University, Kaifeng 475004, China

³Institute of Applied Ecology, Chinese Academy of Sciences, Shenyang 110016, China

⁴Centre for Carbon, Water and Food, School of Life and Environmental Sciences, University of Sydney, Camden NSW 2570, Australia

⁵College of Environmental and Resource Sciences, Dalian Minzu University, Dalian 116600, China

⁶College of Life Sciences, Shenyang Normal University, Shenyang 110034, China

⁷College of food, Shenyang Normal University, Shenyang 110034, China

Received 4 September 2018

Accepted 9 September 2019

Abstract: In this study, the mean temperature of June to July was reconstructed for the period of 1880 to 2014 by using the *Larix gmelinii* tree-ring width data for the Mangui region in the northern Daxing’an Mountains, China. The reconstruction accounts for 43.6% of the variance in the temperature observed from AD 1959–2014. During the last 134 years, there were 17 warm years and 17 cold years, which accounted for 12.7% of the total reconstruction years, respectively. Cold episodes occurred throughout 1887–1898 (average value is 14.2°C), while warm episodes occurred during 1994–2014 (15.9°C). Based on this regional study, the warmer events coincided with dry periods and the colder events were consistent with wet conditions. The spatial correlation analyses between the reconstructed series and gridded temperature data revealed that the regional climatic variations were well captured by this study and the reconstruction represented a regional temperature signal for the northern Daxing’an Mountains. In addition, Multi-taper method spectral analysis revealed the existence of significant periodicities in our reconstruction. Significant spectral peaks were found at 29.7, 10.9, 2.5, and 2.2 years. The significant spatial correlations between our temperature reconstruction and the El Niño–Southern Oscillation (ENSO), Pacific Decadal Oscillation (PDO) and Solar activity suggested that the temperature in the Daxing’an Mountains area indicated both local-regional climate signals and global-scale climate changes.

Keywords: *Larix gmelinii*, Tree rings, temperature reconstruction, El Niño–Southern Oscillation, Pacific Decadal Oscillation, Solar activity.

1. INTRODUCTION

The rise in global temperatures since the 20th century has a significant impact on human activities (Esper *et al.*, 2002; Moberg *et al.*, 2005; IPCC, 2014), resulting in temperature changes at both local-regional and global scales, with a strong influence on upland as well as hydrophytic ecosystems (Cao and Woodward, 1998; Shaver *et al.*, 2000). Warming is expected to have significant effects on ecosystems at high latitudes, where plant growth is mainly limited by temperature (Kittel *et al.*, 2000). The Daxing'an Mountains (DM), which are ranging in the northeast across 200–300 km from east to west and extend over 1220 km from south to north, are one of the most sensitive areas to temperature variation of China (Ding *et al.*, 1994; Wang *et al.*, 1998; Zhang *et al.*, 2016). Previous studies showed that temperature change in this region was linked with solar activities and global land-sea atmospheric circulation. The temperature will rise or fall with the intensity or weakness of solar activity (e.g. the warm period in Middle Ages and the cold period in “Little Ice Age”) (Lean and Rind, 1999; Bond *et al.*, 2001; Herrera *et al.*, 2015).

In recent years, the temperature in northeast China has gradually increased, and the temperature in the growing season has risen significantly (Li and Gong, 2006). To understand the potential impacts of climate variation in this region, it is necessary to thoroughly understand the long-term changes and trends of climate over the last hundred years (Esper *et al.*, 2002; Zhang *et al.*, 2003). However, the historical and instrumental meteorological records are very limited before the 1950s. This poses the most significant impediment to comprehending the processes and mechanisms of past climatic fluctuations in this region (Bao *et al.*, 2012). Thus, understanding the characteristics of long-term paleoclimate records are of great research value for the Daxing'an Mountains, which is fundamental for the prediction of future climate.

Over the past few years, the dendrochronological research has made significant progress in China, such as dendroecological research by Song *et al.*, 2011, Yu *et al.*, 2018; dendrogeomorphological research by Malik *et al.*, 2013, 2017. Besides, because the tree-rings are high-resolution climate proxies containing rich climatic information, from which long paleoclimatic records can develop (Shao *et al.*, 2010). This method has been used to extend limited meteorological data and predicts the impacts of various factors over time in various locations around the world (Pederson *et al.*, 2001; Mann *et al.*, 2009; Cook *et al.*, 2010; Davi *et al.*, 2010; Bao *et al.*, 2012; PAGES 2k Consortium, 2013; Pathi *et al.*, 2017). In recent years, some climate reconstruction projects based on tree rings have also been carried out in the northern Greater Khingan Mountains (Liu *et al.*, 2009; Zhang *et al.*, 2011, 2013; Chen *et al.*, 2012; Yu *et al.*, 2012). However, to date, temperature reconstruction based on tree-ring records were still insufficient in the

northern Greater Khingan Mountains (Zhang *et al.*, 2013). Thus, this lack must be addressed. Mangui (the site codes MG) is situated in the northern Daxing'an Mountains. A large area of natural temperate old-growth forests in this location provides an excellent opportunity for the study of dendroclimatology, which will allow us to better understand the historical and current climate changes in the northern Daxing'an Mountains region.

This paper uses tree-ring data for *Larix gmelinii* in Mangui to (1) reconstruct and investigate temperature variability since AD 1880 based on the tree-ring widths from MG, and (2) explore the potential linkages between the reconstructed June-July temperature data and large scale climatic change.

2. MATERIALS AND METHODS

Study area and sample collection

Our study area is located in Mangui in the northern Daxing'an Mountains, Inner Mongolia Autonomous Region, China (Fig. 1). The region experiences a temperate continental monsoon climate, which is characterized by a long and cold winter, windy and dry spring, short and rainy summer, and cool and frosty autumn (Wu *et al.*, 2004). The average annual temperature is -5.7°C , and the annual total precipitation varies from 320 mm to 690 mm, the growing season is from May to September. The slope of the sample site, MG (890 m a.s.l, $52^{\circ}12'N$ and

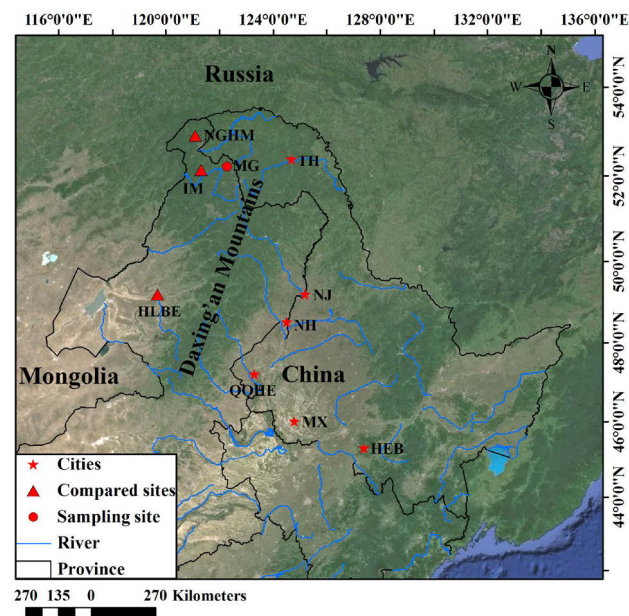


Fig. 1. Location of the sampling site (MG). Northern Greater Hignnan Mountains (HGHM) (Zhang *et al.*, 2013), Inner Mongolia (IM) (Zhang *et al.*, 2011) and Hulunbuir (HLBE) (Shi *et al.*, 2015) were u asterisk sed for comparison. The cities TH(Tahe), NJ (Nenjiang), NH(Nehe), QQHE(Qiqihar), MX(Maoxing) and HEB (Haerbin) were marked with asterisk.

122°17'E), was from 5° to 10°, and the aspect was south. To minimize non-climatic influences on tree growth, the selected stands of *Larix gmelinii* were naturally established, only healthy *Larix gmelinii* with no evidence of recent fire, or human disturbance were selected for sampling at breast height. To collect samples that contained consistent climate signals, the elevations difference between the trees of the sample site was within 40 m. One or two tree-ring increment cores were extracted in North-South directions from each tree (In general, two tree cores were taken in each tree, but in some cases, the collected tree core was damaged and discarded, so only one tree core was utilized). In total, 42 cores from 26 *Larix gmelinii* trees were collected from MG in October 2014.

Development of ring-width chronologies

All cores were preprocessed, air-dried, mounted on the wooden holders using conventional dendrochronological techniques, and subsequently were carefully polished with successively finer grit sandpaper in the laboratory (Fritts, 1976; Holmes, 1983; Cook, 1985). The tree rings were all visually cross-dated with a binocular microscope, annual ring widths were subsequently carefully measured to the nearest 0.001 mm by using a Velmex measuring system. The quality control of cross-dating and measurements was checked by using the COFECHA programme (Holmes, 1983). Each individual ring-width series were detrended in order to remove age-related, non-climatic growth trends (Fritts, 1976). A negative exponential curve or straight line was applied to preserve as much low-frequency signal as possible (Cook, 1990). In a few cases, a cubic spline with 67% of the series length was employed when anomalous low-frequency growth trends occurred. The detrended data from individual tree cores were combined into the site chronology by using a bi-weight robust mean method to minimize the influence of extreme values, outliers or bias in tree-ring indices (Cook, 1990). Three kinds of chronologies were generated from ARSTAN: residual (RES), autoregressive (ARS) and standard (STD). The STD chronology was used for further analyses because it includes both low- and high-frequency signals. We limited our analyses to the period with an EPS of at least 0.85 to determine the length of credible chronology (Cook and Briffa, 1990; Wigley *et al.*, 1984).

Climate data

There is no weather station near the sample sites. As such, the interpolated values, based on records from randomly selected 120 of 164 meteorological stations, were used for growth-climate response analysis. (120 weather stations in northeast China were from Chinese Meteorological Data Sharing Service System (<http://cdc.cma.gov.cn>), another 44 weather stations in Russia from Global Historical Climatology Network (<https://www.ncdc.noaa.gov>). Meteorological records

from a large number of different stations, can reduce the random components or small-scale noise and enhance the reliability of statistical relationships between tree-ring widths and climate data (Pederson *et al.*, 2001).

This interpolation method begins by fitting a partial thin-plate smoothing spline model, that is based on relating location and elevation to ground-based observations to estimate a trend surface, and then a simple kriging procedure was employed to the residuals for trend surface correction (Huang *et al.*, 2013; Li *et al.*, 2014). Analysis of regression was conducted between measured and interpolated precipitations and temperatures at the remaining 44 weather stations, to assess the reliability of the interpolated values. There was a high correlation with $R^2 = 0.99$.

Correlation coefficients between tree-ring width indices and climatic variables from 1959 to 2014 were analyzed by using the data of monthly mean temperature and precipitation. Four climate variables were applied for the dendroclimatological analyses, including monthly total precipitation (Prec), monthly maximum temperature (T_{\max}), monthly mean temperature (T_{mean}) and monthly minimum temperature (T_{\min}). The climate data from the previous June to the current September was used for the correlation analysis.

Global-scale climate variables such as El Niño-Southern Oscillation index (ENSO) and the Pacific Decadal Oscillation index (PDO) (<http://climexp.knmi.nl>) were also used to assess the tree-ring based climatic signals.

Statistical analyses

Pearson correlation function and growth-climate response analyses (Blasing *et al.*, 1984; Biondi and Waikul, 2004) were utilized to identify the most accepted model for the climatic reconstruction. Subsequently, a simple linear regression equation between the tree-ring width and the climate variables was computed for the calibrated period of 1959–2014. The parameters for calibration and verification included the Pearson's correlation coefficient (r), explained variance (r^2), reduction of error (RE), coefficient of efficiency (CE), sign test (ST) and product means test (PMT). All statistical analyses were performed by using commercial software, SPSS12.0 (SPSS, Inc., Chicago, IL, USA).

Power spectral analysis was applied to identify reasonable periodicities and performed over the full range of the reconstruction. The spectral properties of the reconstruction series were assessed by using a multi-taper method. In addition, Spatial correlations between the reconstructed $T_{\text{mean}6-7}$ and the CRU TS 4.01 gridded T_{mean} dataset (45–52°N, 118–127°E) during the common period of 1960–2013 were analyzed by using the KNMI climate explorer (<http://climexp.knmi.nl>). This was done to evaluate the spatiotemporal representativeness of the reconstruction.

3. RESULTS

Chronology Statistics

The chronology statistics are shown in **Table 1**. The mean ring width ranged between 0.75 and 1.56 mm. Mean sensitivity (MS), which indicates the relative difference between adjacent rings, was 0.24, reflecting that tree growth was sensitive to the changes of the local environment. The standard deviation (SD) value was 0.26. The first-order autocorrelation among the tree-ring series was 0.60, indicating that tree growth in the current year had a strong influence on growth in the next year (Fritts, 1976). The value of inter-series correlation was 0.60, with a signal-to-noise ratio of 27.60, suggesting that the chronologies recorded adequate environmental signals. The variance in the first eigenvector accounted for 42.0% in the standard chronology. An expressed population signal (EPS) threshold value of 0.85 was used to assess the most credible period of the chronology to ensure the reliability and validity of the reconstruction. The threshold corresponded to a sample depth of three trees and allowed for the reconstruction of the period of 1880–2014.

The relationship between climate and tree-ring width

The results of correlation between the MG chronology (STD) and the climatic data revealed that tree-ring width indices were negatively correlated to monthly mean temperatures in almost all months (**Fig. 2**); the correlations were significant in July of the prior year as well as March and from June to July of the current year ($P < 0.05$), with the highest correlation coefficient in July of the current year ($r = -0.46$, $P < 0.05$) (**Fig. 2**). Meanwhile, **Fig. 2** show there were significant positive correlations between tree-ring index and the June T_{min} of the previous year. In addition, *Larix gmelinii* radial growth in Mangui was positively correlated with precipitation during current June to July, with significant correlation observed in July (**Fig. 2**). After examining different combinations of

months, the best correlation was confirmed between the ring-width indices and monthly mean temperature from current year June to July. Therefore, we reconstructed monthly mean temperature from June to July of the current year by using the MG chronology.

Development of the regression model

Based on the results of correlation analysis, a linear regression model was used in our study to describe the connection between the tree-ring width and the June-July temperatures. The model was designed as follows:

$$T_{\text{mean6-7}} = 19.14 - 4.03 \times X_t \quad (3.1)$$

($N=55$, $R^2=0.436$, $R^2_{\text{adj}}= 0.426$, $F= 35.29$, $p < 0.0001$)

where $T_{\text{mean6-7}}$ is the mean temperature from June to July of the current year and X_t is the ring-width index of the MG chronology at the t year.

For the calibration period (1959–2014), the reconstruction accounted for 43.6% of the actual $T_{\text{mean6-7}}$ (**Fig. 3**), after adjusting for the loss of degrees of freedom, it still explained 42.6% of the total temperature variance. The method of split-sample was employed to check the stability and reliability of the regression model (1) (Liu *et al.*, 2009). Statistics of calibration and verification were shown in **Table 3**. All calibration and verification parameters were statistically significant ($p < 0.05$), which indicated that the reconstructed equation was acceptable (Fritts, 1976). In addition, the positive CE and RE values (**Table 2**) revealed that model (1) was stable and suitable for further temperature reconstruction (Cook *et al.*, 1999). Significant results of PMT and ST showed a good agreement between the reconstructed and actual data. These analyses suggested that the regression model was valid for temperature reconstruction.

Table 1. Statistical features of STD chronology.

Statistic	STD
Mean sensitivity	0.23
Standard deviation	0.26
First order autocorrelation	0.60
Mean correlation within trees	0.60
Variance in first eigenvector (%)	42.0
Signal-to-noise ratio (SNR)	27.6
Mean ring width (mm)	1.16
Expressed population signal (EPS)	0.91
First year where SSS>0.85 (number of trees)	1880 (3)

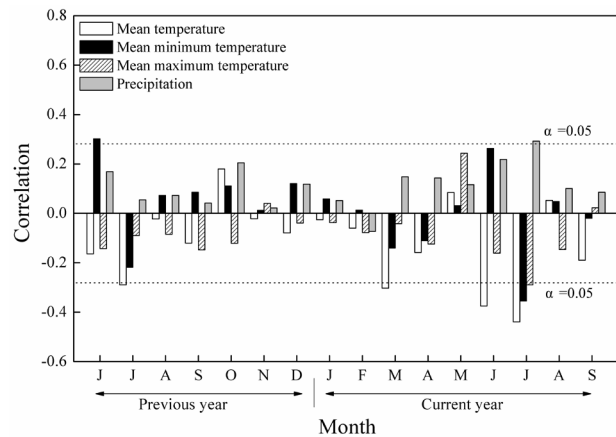


Fig. 2. Correlation coefficients between the monthly climate variables and tree-ring indices for 1959–2014.

Table 2. Statistics of calibration and verification test for the common period of 1959–2014.

Calibration	R	R ²	Verification	R	Reduction of error	Coefficient of efficiency	Sign test	Product means test
Whole section 1959–2014	0.66 ^a	0.436 ^a						
Front section 1959–1983	0.53 ^a	0.28 ^a	Back section 1984–2014	0.71 ^a	0.61 ^a	0.35 ^a	(26+ / 5-) ^a	2.8 ^a
Back section 1984–2014	0.71 ^a	0.50 ^a	Front section 1959–1984	0.53 ^a	0.61 ^a	0.43 ^a	(21+ / 5-) ^a	3.3 ^a

^a Significant at the 0.05 level

Table 3. Rank of years of warm/cold reconstructed mean temperature from June to July ($T_{\text{mean6-7}}$).

Rank	Warm year	$T_{\text{max6-7}}$ RECHT89 (°C)	Cold year	$T_{\text{max6-7}}$
1	2008	17.28	1888	12.66
2	2003	16.85	1893	13.21
3	2012	16.67	1902	13.22
4	1994	16.65	1932	13.33
5	2014	16.59	1898	13.42
6	1954	16.46	1880	13.60
7	2011	16.43	1991	13.62
8	2004	16.38	1934	13.72
9	1886	16.36	1882	13.73
10	1885	16.28	1892	13.81
11	1975	16.26	1978	13.91
12	1967	16.15	1891	13.94
13	1919	16.14	1895	14.04
14	1883	16.13	1958	14.05
15	2001	16.11	1890	14.05
16	2005	16.09	1927	14.10
17	1939	16.07	1900	14.15

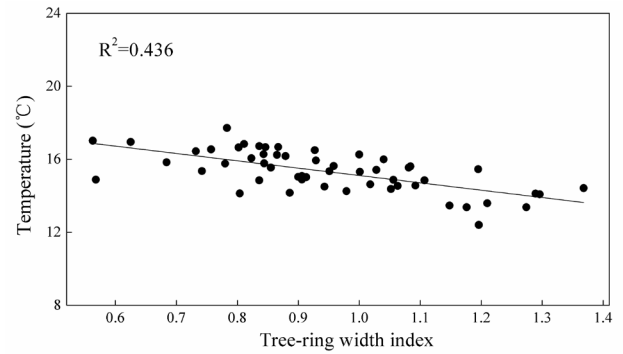
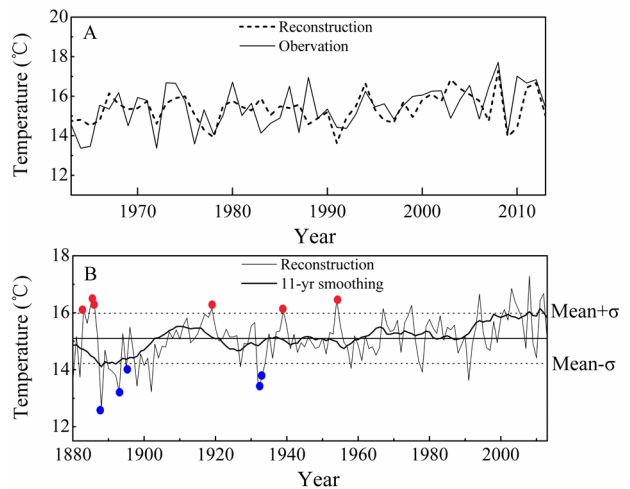
Temperature variations from AD 1880 to 2014

Based on model (1), the mean temperature that was reconstructed from 1880 to 2014 for the MG region exhibited a mean of 15.1°C and a standard deviation of $\sigma = 0.88^\circ\text{C}$. We defined years with values $> \text{mean} + 1\sigma$ as a warm year, and values $< \text{mean} - 1\sigma$ as a cold year. During the last 134 years, there were 17 warm years, 17 cold years, which accounted for 12.7% of the total reconstruction years, respectively (Table 3). The decadal variability was highlighted by using an 11-year moving average to the reconstruction (Fig. 4B). The warm periods and cold periods can be distinguished. Cold periods occurred in 1887–1898 (average value is 14.2°C), while warm periods occurred in 1994–2014 (15.9°C) (Fig. 4B). Furthermore, there are two obvious processes of mean temperature increasing in 1888–1910 (from 14.1 to 15.5°C, and lasting for 23 years), 1987–2012 (from 15.1 to 16.2°C, and lasting for 26 years).

4. DISCUSSION

Tree growth-climate responses

In this study, summer (June to July) temperatures were the most significant negative correlations with the

**Fig. 3.** Scatter plot of the tree-ring width index and the averaged $T_{\text{mean6-7}}$ from June to July (1959–2014).**Fig. 4.** (A) Comparison of actual and reconstructed $T_{\text{mean6-7}}$ from 1959 to 2014 and (B) the reconstructed June-July temperature series since 1880. The smoothed line indicates the 11-year moving average, and red dots represent drought events, blue dots represent flood events.

annual radial growth of *Larix gmelinii* at MG region (Fig. 2). Similar results were also obtained by studies of other tree species in various areas of China (Bao *et al.*, 2012; Gao *et al.*, 2013; Lu *et al.*, 2016; Shi *et al.*, 2013; Tian *et al.*, 2009). The hot summer temperatures might limit the growth of *Larix gmelinii* due to the increased water deficits caused by the enhanced forest respiration and evaporation of soil moisture (Huang *et al.*, 2010; Zhang *et al.*, 2010). According to the climatic data of the study area from 1959 to 2014, the mean temperature from June to

July was significantly negatively correlated with the average precipitation ($r = -0.68$, $P < 0.001$), indicating that the effect of precipitation on the growth of *Larix gmelinii* trees in the high-temperature season was significant. In this study area, soil water is mainly used by trees during the period from June to August, especially in July when the temperature is highest in a year (Bai *et al.*, 2011). The highest precipitation occurs in July–August, but the maximum temperature occurs from June–July (Fig. 5). During this period, the increase in water demand due to transpiration may result in a deficit of soil moisture. Soil moisture evaporation was greater than precipitation, and therefore moisture requirements for growth cannot be met. Our results also revealed that the influence of mean temperatures was more significant than the influence of precipitation during the current June–July. In addition, low temperatures in previous and current June had a great limitation on tree-ring formation. The higher the T_{\min} in June, the earlier the growth begins, and the longer the growing season, resulting in a wider annual ring (Wu and Shao, 1996). The radial growth of tree rings

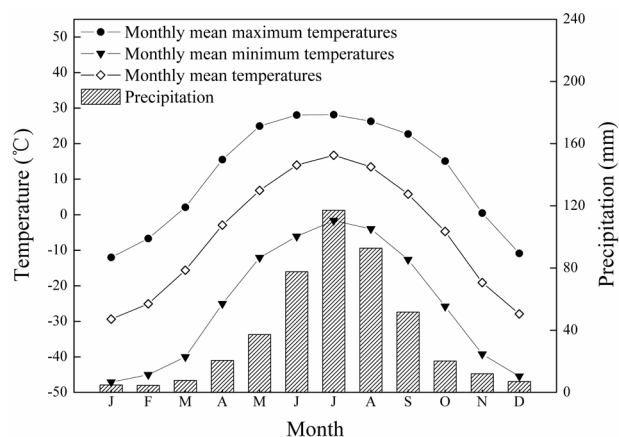


Fig. 5. Mean monthly temperature (in °C) and total precipitation (in mm) at Mangui (MG) in the northern Daxing'an Mountains (AD 1959–2014) based on interpolated values from 164 climate stations.

is affected by the amount of stored compounds. The higher T_{\min} in June of the previous year may enhance photosynthetic production and store more carbohydrates for the next summer (DeLucia and Smith, 1987). Our results are in line with those of Wang *et al.*, 2005, who suggested that the annual growth of *Larix gmelinii* trees in Mohe was positively correlated with the T_{\min} in June, indicating that trees respond to climate with regional homogeneity.

Regional- to large-scale comparison

Drought is not only due to lower precipitation but also to higher temperatures. Under normal rainfall conditions, high temperatures can cause severe droughts, and precipitation is accompanied by low temperatures (Yi *et al.*, 2012; Bao *et al.*, 2012). Historical literature evidence shows that many drought and flooding events occurred in Heilongjiang Province after AD 1880 (Wen and Sun, 2007). The high-temperature years that occurred in AD 1883, 1885, 1886, 1919, 1939, and 1954 were linked with drought events (Table 4) and low-temperature years of 1888, 1892, 1895, 1932 and 1934 were associated with the wet events in the study region (Table 4).

To further evaluate the reliability of this reconstruction, we compared the reconstructed series with nearby tree-ring-based reconstruction temperature series by Zhang *et al.*, 2013 (the site codes NGHM, 680 m a. s. l., 52°55' N, 121°06' E; 193 km from our sampling point), Zhang *et al.*, (2011) (the site codes IM, 51°03'15"–52°08'08" N, 120°00'20" – 121°19'21" E; 120 km from our sampling point) and reconstruction Palmer drought severity index (PDSI) series by Shi *et al.*, 2015 (the site codes HLBE, 515–669 m a. s. l., 49°12' N, 119°42' E; 607 km from our sampling point) (Fig. 1, Fig. 6). A significant negative correlation ($r = -0.43$, $p < 0.001$) between our reconstruction and the May–July PDSI reconstruction in HLBE (Fig. 6d) was found, while our reconstruction of $T_{\text{mean}6-7}$ had similar variations in the May–October temperature reconstruction in NGHM ($r=0.35$, $p<0.01$; Fig. 6c) and May–September tempera-

Table 4. The dry/wet years of the reconstructed temperature for the Mangui (MG) region in comparison with historical documents (Wen and Sun, 2007).

Dry and wet years	Short description of weather or related events
1883	Heilongjiang: Severe drought occurred in 27 regions in summer, such as Qiqihar, Haerbin, Moergen (now Nenjiang), Maoxing, Ningguta, etc.
1885	Heilongjiang: Drought occurred in summer, such as Heilongjiang city, Moergen (now Nenjiang), Qiqihar, Sanxing (now Yilan), Ningguta, etc.
1886	Heilongjiang: Drought occurred in summer, such as Heilongjiang City, Qiqihar, Moergen (now Nenjiang), Maoxing, Ningguta, etc.
1919	Heilongjiang: Drought occurred in summer, such as Haerbin, Tonghe, Qiqihar, Xibuteha (now Zhalantun), Nehe, Anda, Zhaozhou, etc.
1939	Heilongjiang: Severe drought occurred in Jiamusi in summer.
1954	Heilongjiang: Drought occurred in summer, such as, Nenjiang, Shangzhi, Tieli, Suiling, Hailun, Nenjiang, etc.
1888	Heilongjiang: Flooding disaster occurred in 27 regions in summer, such as Qiqihar, Moergen (now Nenjiang), Maoxing, etc.
1892	Heilongjiang: Flooding disaster occurred in 20 regions in summer, such as Qiqihar, Maoxing, Wuchang, etc.
1895	Heilongjiang: Flooding disaster occurred in summer, such as Heilongjiang City, Hulan, Boduna, Haerbin, etc.
1932	Heilongjiang: Severe flooding disaster occurred in summer, such as Zhanlantun, Qiqihar, Haerbin, Tahe, Zhaodong, Dongning, etc.
1934	Heilongjiang: Flooding disaster occurred in summer, such as Anda, Qiqihar, Haerbin, Nenjiang, Hulan, etc.

ture reconstruction in IM ($r = 0.31$, $p < 0.01$; **Fig. 6b**). The results showed that despite some differences in these reconstructions, similar temperature patterns were found during 1880–1885, 1888–1906, 1925–1933, 1943–1947, 1953–1964 and 1980–2008 in these areas, (**Fig. 6**), indicating regional climate change.

The results showed that the large-scale regional temperature variations had been well captured by our reconstruction, which was significantly positively correlated with regional gridded temperatures (**Fig. 7**). The above results showed that our reconstruction could capture the temperature signals well. Thus, the reconstruction preserved valid information about regional climate change and provided a valuable profile of past climatic variation in this region.

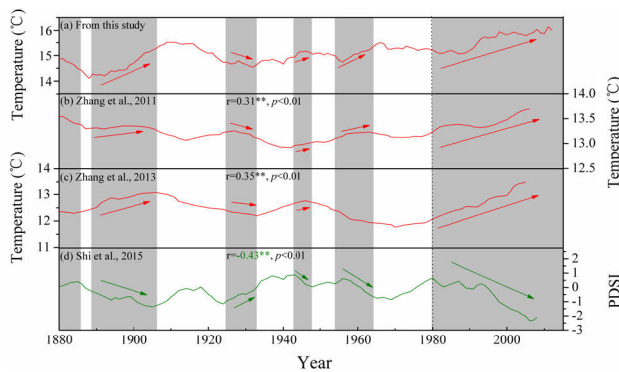


Fig. 6. Comparison of June–July mean temperature reconstruction in MG with other tree-ring proxies from surrounding areas: (a) June–July maximum temperature reconstruction in this study; (b) May–September temperature reconstruction in Inner Mongolia (Zhang *et al.*, 2011); (c) May–October temperature reconstruction in northern Greater Hignnan Mountains, China (Zhang *et al.*, 2013); (d) Annual PDSI reconstruction from tree-ring of Mongolian pine in Hulunbuir, Northeast China (Shi *et al.*, 2015). The gray areas mean the common warm/cold periods.

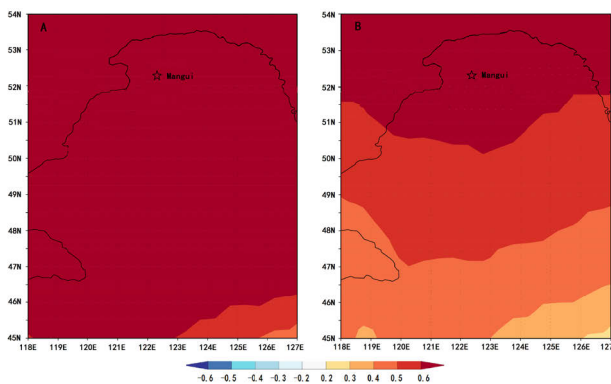


Fig. 7. Spatial correlation of (A) instrumental and (B) reconstructed June–July temperatures with regional gridded June–July temperatures during the period 1959–2014. The asterisk mark in is the sampling position.

Possible forcing mechanism

The multi-taper method (MTM) of spectral analysis (Wei, 2010) revealed that the reconstructed $T_{\text{mean}6-7}$ exhibited significant cycles, which indicated that the $T_{\text{mean}6-7}$ in MG region could be affected by other factors. Significant peaks of 2.5, and 2.2 years were observed (**Fig. 8**). The 2–7 years peak cycle was found in some temperature-related reconstruction by tree-rings in the northeast of China (Bao *et al.*, 2012; Liu *et al.*, 2013), which were within the range of the ENSO cycle (Allan *et al.*, 1996; Su and Wang, 2007; Hocke, 2009; Gergis and Fowler, 2009). A possible connection between $T_{\text{mean}6-7}$ variability and the ENSO was supported by the significantly positive correlations between the reconstructed $T_{\text{mean}6-7}$ and sea surface temperatures (SSTs) in the eastern equatorial Pacific Ocean (**Fig. 9**). Some studies have suggested that ENSO had a strong influence on the strength of East Asian Summer Monsoon (EAWM) (Zhang *et al.*, 1999; Wu and Wang, 2002; Lu, 2005). Mangui is located at the boundary zone of the East Asia Summer Monsoon (EASM) (Yang, *et al.*, 1992; Li and Zeng, 2003). The East Asia Summer Monsoon climate regimes dominate the fecundity or deficit of water availability, and trends in temperature (Zhu *et al.*, 2009; Li *et al.*, 2009; Chen *et al.*, 2011, 2012; Gao *et al.*, 2013), the annual warm summers are related to weaker summer East Asia monsoon climate (Zhu *et al.*, 2009; Li *et al.*, 2009). In other words, the stronger the monsoon is, the lower the summer temperature is, and vice versa. The cycles of 10.9-years may suggest the impact of solar effects, such as sunspot activity (Stuiver and Braziunas, 1993; Grootes and Stuiver, 1997; Yi *et al.*, 2012), which was supported by the significant positive correlations of the reconstructed $T_{\text{mean}6-7}$ with the number of sunspots (<http://www.sidc.be/silso/datafiles>) from June to July of the current year, with a correlation coefficient of 0.215 ($N = 135$, 1880–2014, $p = 0.009$).

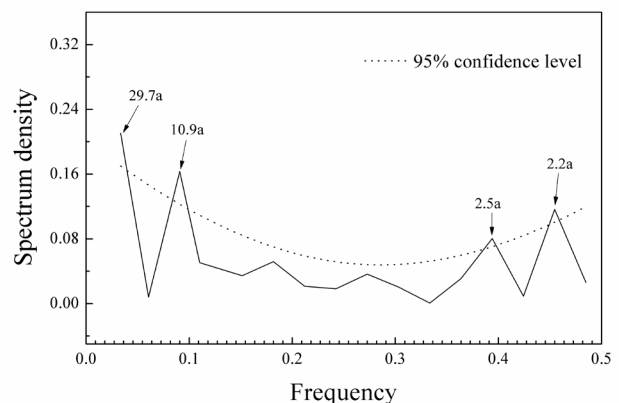


Fig. 8. The power spectrum analyses of reconstructed June–July mean temperature.

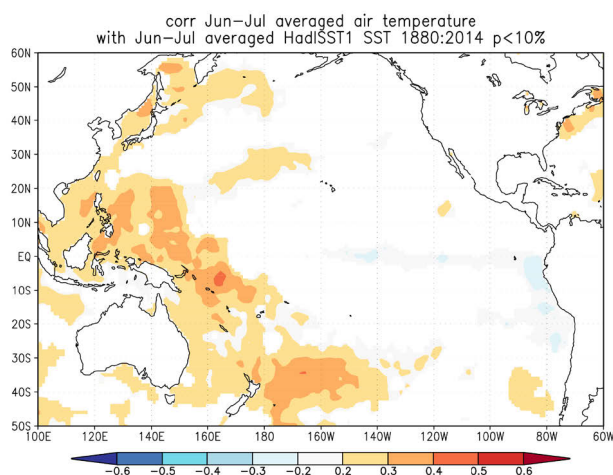


Fig. 9. Spatial correlation for the reconstruction with June–July averaged HadISST1 SST during the period of 1880–2014.

The significant spectral peaks at 29.7-yr (Fig. 8) was possibly linked with the 15–30 yr periods of the Pacific Decadal Oscillation (PDO) (Minobe, 1999; Gedalof *et al.*, 2002; Ma, 2007), which was supported by the significant positive correlations of the reconstructed $T_{\text{mean}6-7}$ with SSTs in the western Pacific Ocean (Fig. 9) and with the annual PDO (MacDonald and Case 2005), with $R^2 = 0.156$ ($N = 117$, $p < 0.05$; 1880–1996). Some other tree-ring studies closed to our study region, discovered that the *Hailar pine*, *Larix gmelinii* and tree-ring widths are also significantly correlated with the PDO (Chen *et al.*, 2011, 2012; Bao *et al.*, 2015).

As mentioned above, the complex connections with the ENSO, PDO and Solar activity suggested that the temperature in the Mangui area indicated both local-regional climate signals and global-scale climate changes.

CONCLUSION

The mean temperature from June to July was reconstructed for the period of 1880 to 2014 by using tree-ring data from MG in the northern Daxing'an Mountains, China. The reconstructed temperature series provided essential information concerning temperature variations in this region. During the last 134 years, there were 17 warm years, 17 cold years, which accounted for 12.7% of the total reconstruction years, respectively. Cold episodes occurred in the intervals 1887–1898, while warm episodes occurred in 1994–2014. In and near the study region, the warmer events coincided with dry periods and the colder events consistent with wet conditions. The spatial correlation analyses between the reconstruction series and gridded temperature data revealed that the regional climatic variations were well captured by this study and the reconstruction represented a regional temperature signal for the northern Daxing'an Mountains. In addition, multi-taper method spectral analysis revealed

the existence of significant periodicities in our reconstruction. Significant spectral peaks were found at 29.7, 10.9, 2.5, and 2.2 years. The significant spatial correlations between our temperature reconstruction and the El Niño–Southern Oscillation (ENSO), and Pacific Decadal Oscillation (PDO) and Solar activity suggested that temperature variability in the Mangui area was probably driven by extensive large-scale atmospheric-oceanic variability and solar activity.

ACKNOWLEDGEMENTS

The research was funded by the National Natural Science Foundation of China (Nos. 41330530, 41430639 and 41575153).

REFERENCES

- Allan R, Lindsay J and Parker D, 1996. El Niño: Southern Oscillation and Climatic Variability. Commonwealth CSIRO Publishing, Melbourne, Australia.
- Bai, XF, H Han, FY Zhou, RS Zhang, GJ Zhao and JH Liu, 2011. Study on ecological characteristics of transpiration and water consumption of *Pinus sylvestris* var. *mongolica* in sand. *Journal of Liaoning Technical University (Natural Science)* 30(3): 404–407. (In Chinese with English abstract).
- Bao G, Liu Y and Linderholm HW, 2012. April–September mean maximum temperature inferred from Hailar pine (*Pinus sylvestris* var. *mongolica*) tree rings in the Hulunbuir region, Inner Mongolia, back to 1868 AD. *Palaeogeography, Palaeoclimatology, Palaeoecology* 313(1): 162–172, DOI 10.1016/j.palaeo.2011.10.017.
- Bao G, Liu Y and Liu N, 2015. Drought variability in eastern Mongolian Plateau and its linkages to the large-scale climate forcing. *Climate Dynamics* 44(3–4): 717–733, DOI 10.1007/s00382-014-2273-7.
- Biondi F and Waikul K, 2004. DENDROCLIM2002: A C++ program for statistical calibration of climate signals in tree-ring chronologies. *Computers and Geosciences* 30(3): 303–311, DOI 10.1016/j.cageo.2003.11.004.
- Blasing TJ, Solomon AM and Duvick DN, 1984. Response functions revisited. *Tree-Ring Bulletin* 44: 1–15.
- Bond G, Kromer B, Beer J, Muscheler R, Evans MN, Showers W, Hoffmann S, Lotti-Bond R, Hajdas I and Bonani G, 2001. Persistent Solar Influence on North Atlantic Climate During the Holocene. *Science* 294: 2130–2136, DOI 10.1126/science.1065680.
- Cao M and Woodward FI, 1998. Dynamic responses of terrestrial ecosystem carbon cycling to global climate change. *Nature* 393(6682): 249–252, DOI 10.1038/30460.
- Chen Z, He X and Cook ER, 2011. Detecting dryness and wetness signals from tree-rings in Shenyang, Northeast China. *Palaeogeography, Palaeoclimatology, Palaeoecology* 302(3): 301–310, DOI 10.1016/j.palaeo.2011.01.018.
- Chen Z, Zhang X and Cui M, 2012. Tree-ring based precipitation reconstruction for the forest–steppe ecotone in northern Inner Mongolia, China and its linkages to the Pacific Ocean variability. *Global and Planetary Change* 86–87(4): 45–56, DOI 10.1016/j.gloplacha.2012.01.009.
- Cook ER, 1990. Methods of Dendrochronology: Applications in Environmental Science.
- Cook ER, 1985. *A time series approach to tree-ring standardization*. Ph.D. Thesis, University of Arizona, Tucson, AZ, USA
- Cook ER and Briffa KR, 1990. *Data analysis*. In *Methods of Dendrochronology*; Cook, E.R., Kairiukstis, L.A., Eds.; Kluwer: Boston, MA, USA pp. 97–162
- Cook ER, Anchukaitis KJ and Buckley BM, 2010. Asian monsoon failure and megadrought during the last millennium. *Science* 328(5977): 486–489, DOI 10.1126/science.1185188.

- Cook ER, Meko DM, Stahle DW and Cleaveland MK, 1999. Drought reconstructions for the continental United States. *Journal of Climate* 12: 1145–1162, DOI 10.1175/1520-0442(1999)012<1145:DRFTCU>2.0.CO;2.
- Davi N, Jacoby G and Fang K, 2010. Reconstructing drought variability for Mongolia based on a large scale tree ring network: 1520–1993. *Journal of Geophysical Research Atmospheres* 115(D22): 1842–1851, DOI 10.1029/2010JD013907.
- DeLucia EH and Smith WK, 1987. Air and soil temperature limitations on photosynthesis in Engelmann spruce during summer. *Canadian Journal of Forest Research* 17: 527–533, DOI 10.1139/x87-088.
- Ding YH and Dai XS, 1994. Temperature variation in China during the last 100 years. *Meteorology* 12: 19–26 (in Chinese).
- Esper J, Cook ER and Schweingruber FH, 2002. Low-frequency signals in long tree-ring chronologies for reconstructing past temperature variability. *Science* 295: 2250–2253, DOI 10.1126/science.1066208.
- Fritts HC, 1976. *Tree Rings and Climate*. Academic Press: New York, NY, USA
- Holmes RL, 1983. Computer-Assisted Quality Control in Tree-Ring Dating and Measurement. *Tree-Ring Bulletin* 44(3): 69–75.
- Gao J, Shi Z and Xu L, 2013. Precipitation variability in Hulunbuir, northeastern China since 1829 AD reconstructed from tree-rings and its linkage with remote oceans. *Journal of Arid Environments* 95(8): 14–21, DOI 10.1016/j.jaridenv.2013.02.011.
- Gedalof Z, Mantua NJ and Peterson DL, 2002. A multi-century perspective of variability in the Pacific Decadal Oscillation: new insights from tree rings and coral. *Geophysical Research Letters* 29(24): 57–51, DOI 10.1029/2002GL015824.
- Gergis JL and Fowler AM, 2009. A history of ENSO events since A.D. 1525: implications for future climate change. *Climatic Change* 92(3–4): 343–387, DOI 10.1007/s10584-008-9476-z.
- Groote PM and Stuiver M, 1997. Oxygen 18/16 variability in Greenland snow and ice with 103 to 105-year time resolution. *Journal of Geophysical Research* 102: 26455–26470, DOI 10.1029/97JC00880.
- Herrera VMV, Mendoza B and Herrera GV, 2015. Reconstruction and prediction of the total solar irradiance: From the Medieval Warm Period to the 21st century. *New Astronomy* 34: 221–233, DOI 10.1016/j.newast.2014.07.009.
- Hocke K, 2009. QBO in solar wind speed and its relation to ENSO. *Journal of Atmospheric and Solar-Terrestrial Physics* 71(2): 216–220, DOI 10.1016/j.jastp.2008.11.017.
- Huang C, Zheng X and Tait A, 2013. On using smoothing spline and residual correction to fuse rain gauge observations and remote sensing data. *Journal of Hydrology* 508(2): 410–417, DOI 10.1016/j.jhydrol.2013.11.022.
- Huang J, Tardif JC and Bergeron Y, 2010. Radial growth response of four dominant boreal tree species to climate along a latitudinal gradient in the eastern Canadian boreal forest. *Global Change Biology* 16(2): 711–731, DOI 10.1111/j.1365-2486.2009.01990.x.
- IPCC (Intergovernmental Panel on Climate Change), 2014. Climate change 2014: mitigation of climate change [M/OL]. Cambridge: Cambridge University Press, 2014 [2014-09-10]. <http://www.ipcc.ch/report/ar5/wg3>
- Kittel TGF, Steffen WL and Chapin FSI, 2000. Global and regional modelling of Arctic-boreal vegetation distribution and its sensitivity to altered forcing. *Global Change Biology* 6(S1): 1–18, DOI 10.1046/j.1365-2486.2000.06011.x.
- Lean J and Rind D, 1999. Evaluating sun–climate relationships since the Little Ice Age. *Journal of atmospheric and solar-terrestrial physics* 61(1–2): 25–36, DOI 10.1016/S1364-6826(98)00113-8.
- Li J and Zeng Q, 2003. A new monsoon index and the geographical distribution of the global monsoons. *Advances in Atmospheric Sciences* 20(2): 299–302.
- Li J, Cook ER and D'Arrigo R, 2009. Moisture variability across China and Mongolia: 1951–2005. *Climate Dynamics* 32(7–8): 1173–1186, DOI 10.1007/s00382-008-0436-0.
- Li J and Gong Q, 2006. Analysis of Temperature Change Characteristics in Summer in Northeast China. *Journal of Meteorology and Environment* 1: 6–10.
- Li T, Zheng X, Dai Y, Yang C, Chen Z, Zhang S and Liao R, 2014. Mapping near-surface air temperature, pressure, relative humidity and wind speed over Mainland China with high spatiotemporal resolution. *Advances In Atmospheric Sciences* 31: 1127–1135, DOI 10.1007/s00376-014-3190-8.
- Liu Y, Bao G and Song H, 2009. Precipitation reconstruction from Hailar pine (*Pinus sylvestris* var. *mongolica*) tree rings in the Hailar region, Inner Mongolia, China back to 1865 AD. *Palaeogeography, Palaeoclimatology, Palaeoecology* 282(4): 81–87, DOI 10.1016/j.palaeo.2009.08.012.
- Liu Y, Wang Y and Li Q, 2013. Reconstructed May–July mean maximum temperature since 1745 AD based on tree-ring width of *Pinus tabulaeformis*, in Qianshan Mountain, China. *Palaeogeography Palaeoclimatology Palaeoecology* 388(19): 145–152, DOI 10.1016/j.palaeo.2013.08.011.
- Lu RY, 2005. Interannual variation of North China rainfall in rainy season and SSTs in the equatorial eastern Pacific. *Chinese Science Bulletin* 50: 2069–2073, DOI 10.1360/04wd0271.
- Lu R, Jia F and Gao S, 2016. Tree-ring reconstruction of January–March minimum temperatures since 1804 on Hasi Mountain, northwestern China. *Journal of Arid Environments* 127: 66–73, DOI 10.1016/j.jaridenv.2015.10.020.
- Ma ZG, 2007. The interdecadal trend and shift of dry/wet over the central part of north China and their relationship to the Pacific Decadal Oscillation (PDO). *Chinese Science Bulletin* 52 (12): 2130–2139, DOI 10.1007/s11434-007-0284-z.
- MacDonald GM and Case RA, 2005. Variations in the Pacific Decadal Oscillation over the past millennium. *Geophysical Research Letters* 32: L08703, DOI 10.1029/2005GL022478.
- Malik I, Tie Y, Owczarek P, Wistuba M, Pilorz W, Woskiewicz-Ślęzak B, 2013. Human-planted alder trees as a protection against debris Human-planted alder trees as a protection against debris flows (a dendrochronological study from the Moxi Basin, Southwestern China). *Geochronometria* 40(3): 208–216, DOI 10.2478/s13386-013-0113-x.
- Malik I, Wistuba M, Tie Y, Owczarek P, Woskiewicz-Ślęzak B and Łuszczynska K, 2017. Mass movements of differing magnitude and frequency in a developing high-mountain area of the Moxi basin, Hengduan Mts, China – A hazard assessment. *Applied Geography* 87: 54–65, DOI 10.1016/j.apgeog.2017.08.003.
- Mann ME, Zhang Z and Rutherford S, 2009. Global signatures and dynamical origins of the Little Ice Age and Medieval Climate Anomaly. *Science* 326(5957): 1256–1260, DOI 10.1126/science.1177303.
- Minobe S, 1999. Resonance in bidecadal and pentadecadal climate oscillations over the North Pacific: Role in climatic regime shifts. *Geophysical Research Letters* 26(7): 855–858, DOI 10.1029/1999GL001119.
- Moberg A, Sonechkin DM and Holmgren K, 2005. Highly variable Northern Hemisphere temperatures reconstructed from low- and high-resolution proxy data. *Nature* 433(7026): 613–617, DOI 10.1038/nature03265.
- PAGES 2 K Consortium, 2013. Continental-scale temperature variability during the past two millennia. *Nature Geoscience* 6: 339–346, DOI 10.1038/NGEO1797.
- Panthi S, Bräuning A, Zhou ZK and Fan ZX, 2017. Tree rings reveal recent intensified spring drought in the central Himalaya, Nepal. *Global and Planetary Change* 157: 26–34, DOI 10.1016/j.gloplacha.2017.08.012.
- Pederson N, Jacoby GC and D'Arrigo RD, 2001. Hydrometeorological Reconstructions for Northeastern Mongolia Derived from Tree Rings: 1651–1995. *Journal of Climate* 14(5): 872–881, DOI 10.1175/1520-0442(2001)014<0872:HRFNMD>2.0.CO;2.
- Shao X, Xu Y, Yin ZY, 2010. Climatic implications of a 3585-year tree-ring width chronology from the northeastern Qinghai-Tibetan Plateau. *Quaternary Science Reviews* 29(17–18): 2111–2122, DOI 10.1016/j.quascirev.2010.05.005.
- Shaver GR, Canadell J and Iii FSC, 2000. Global warming and terrestrial ecosystems: A conceptual framework for analysis. *Bioscience* 50(10): 871–882, DOI 10.1641/0006-3568(2000)050[0871:GWATEA]2.0.CO;2.

- Shi Z, Gao J and Yang X, 2013. Tree-ring based reconstruction of mean maximum temperatures since AD 1829. *Forestry Chronicle* 89(2): 184–191, DOI 10.5558/tfc2013-036.
- Shi Z, Xu L and Dong L, 2015. Growth-climate response and drought reconstruction from tree-ring of Mongolian pine in Hulunbuir, Northeast China. *Journal of Plant Ecology* 9(1): 51–60, DOI 10.1093/jpe/rtv029.
- Song K, Yu Q, Shang KK, Yang TH and Da LJ, 2011. The spatio-temporal pattern of historical disturbances of an evergreen broad-leaved forest in East China: a dendroecological analysis. *Plant Ecology* 212(8): 1313–1325, DOI 10.1007/s11258-011-9907-1.
- Stuiver M and Braziunas T, 1993. Modeling atmospheric ^{14}C influences and ^{14}C ages of marine samples to 10,000 BC. *Radiocarbon* 35: 137–189.
- Su MF and Wang HJ, 2007. Relationship and its instability of ENSO—Chinese variations in droughts and wet spells. *Science In China Series D-Earth Sciences* 50: 145–152, DOI 10.1007/s11430-007-2006-4.
- Tian QH, Gou XH and Yong Z, 2009. May-June mean temperature reconstruction over the past 300 years based on tree rings in the Qilian Mountains of the northeastern Tibetan Plateau. *Iawa Journal* 30(4): 421–434, DOI 10.1163/22941932-90000229.
- Wang LL, Shao XM, Huang L and Liang EY, 2005. Tree-ring characteristics of *Larix gmelinii* and *Pinus sylvestris* var. *mongolica* and their response to climate in Mohe, China. *Acta Phytocool Sin* 29: 380–385.
- Wang SW, Ye JL and Gong DY, 1998. Construction of mean annual temperature series for the last one hundred years in China. *J Appl Meteorol Sci* 9: 392–401 (in Chinese).
- Wei FY, 2010. *Modern Climate Statistics Diagnosis and Forecasting Techniques*. China Meteorological Press, Beijing (in Chinese).
- Wen KG and Sun YG, 2007. The Documents of Chinese Meteorological Disaster: Volume of Heilongjiang Province. Meteorological Publishers, Beijing (in Chinese).
- Wigley TML, Briffa KR and Jones PD, 1984. On the Average Value of Correlated Time Series, with Applications in Dendroclimatology and Hydrometeorology. *Journal of Climatology and Applied Meteorology* 23(2): 201–213, DOI 10.1175/1520-0450(1984)023<0201:OTAVOC>2.0.CO;2.
- Wu R and Wang B, 2002. A Contrast of the East Asian Summer Monsoon-ENSO Relationship between 1962–77 and 1978–93. *Journal of Climate* 15: 3266–3279, DOI 10.1175/1520-0442(2002)015<3266:ACOTEA>2.0.CO;2.
- Wu X and Shao X, 1996. A preliminary study on impact of climate change on tree growth using tree ring-width data. *Acta Geographica Sinica* 1996(S1): 92–101.
- Wu X P, Zhu B and Zhao SQ, 2004. Comparison of community structure and species diversity of mixed forests of deciduous broad-leaved tree and Korean pine in northeast China. *Chinese Biodiversity* 12(1): 174–181.
- Yang G, Chen X and Zhou D, 1992. Ordination and gradient analysis of coniferous forest in Daxinganling. *Journal of Northeast Forestry University* 3(1): 42–47.
- Yi L, Yu H and Ge J, 2012. Reconstructions of annual summer precipitation and temperature in north-central China since 1470 AD based on drought/flood index and tree-ring records. *Climatic Change* 110(1–2): 469–498, DOI 10.1007/s10584-011-0052-6.
- Yu J, Shah S, Zhou G, Xu Z and Liu Q, 2018. Tree-Ring-Recorded Drought Variability in the Northern Daxing'anling Mountains of Northeastern China. *Forests* 9: 674, DOI 10.3390/f9110674.
- Yu S, Wang LL and Jin C, 2012. Reconstructing mean maximum temperatures of May–August from tree-ring maximum density in North Da Hinggan Mountains, China. *Science Bulletin* 57(16): 2007–2014, DOI 10.1007/s11434-012-5055-9.
- Zhang Q, Cheng G and Yao T, 2003. A 2,326-year tree-ring record of climate variability on the northeastern Qinghai-Tibetan Plateau. *Geophysical Research Letters* 30(14): 1739, DOI 10.1029/2003GL017425.
- Zhang RH, Sumi A and Kimoto M, 1999. A diagnostic study of the impact of El Niño on the precipitation in China. *Advances In Atmospheric Sciences* 16: 229–241, DOI 10.1007/BF02973084.
- Zhang T, Yuan Y and Wei W, 2013. Tree-ring-based temperature reconstruction for the northern Greater Hinggan Mountains, China, since A.D. 1717. *International Journal of Climatology* 33(2): 422–429, DOI 10.1002/joc.3433.
- Zhang XL, Cui MX and Ma YJ, 2010. Chronology of the annual ring width of *Larix gmelinii* in the Kudur area of Daxing'anling and its relationship with climate change. *Chinese Journal of Applied Ecology* 21(10): 2501–2507 (In Chinese).
- Zhang X, Bai X and Chang Y, 2016. Increased sensitivity of Dahurian larch radial growth to summer temperature with the rapid warming in Northeast China. *Trees* 30(5): 1799–1806, DOI 10.1007/s00468-016-1413-6.
- Zhang X, He X and Li J, 2011. Temperature reconstruction (1750–2008) from Dahurian larch tree-rings in an area subject to permafrost in Inner Mongolia, Northeast China. *Climate Research* 47(3): 151–159, DOI 10.3354/cr00999.
- Zhang XL, Cui MX and Ma YJ, 2010. *Larix gmelinii* tree-ring width chronology and its responses to climate change in Kuduer, Great Xing'an Mountains. *Chinese Journal of Applied Ecology* 21(10): 2501
- Zhu HF, Fang XQ and Shao XM, 2009. Tree ring-based February–April temperature reconstruction for Changbai Mountain in Northeast China and its implication for East Asian winter monsoon. *Climate of the Past Discussions* 5(2): 661–666, DOI 10.5194/cp-5-661-2009.